# Sulfonated organosilica-aluminum phosphates as useful catalysts for acid-catalyzed reactions: Insights into the effect of synthesis parameters on the final catalyst

**L. Aguado-Deblas, R. Estevez*, F.J. Lopez-Tenllado, D. Luna, F.M. Bautista***

*Departamento de Química Orgánica, Instituto Universitario de Investigación en Química Fina y Nanoquímica (IUNAN), Universidad de Córdoba, Campus de Excelencia Internacional Agroalimentario CeiA3 Edificio Marie Curie, E14014 Córdoba, Spain.*

**E-mail addresses: fmbautista@uco.es (F.M. Bautista); q72estor@uco.es (R.Estevez)*

All correspondence concerning this manuscript should be addressed to:

Prof. Felipa M. Bautista Rubio

Departamento Química Orgánica, Universidad de Córdoba, Campus de Rabanales, Edificio Marie Curie E-14014-Córdoba, España

Fax: (+34)957212066

E-mail: fmbautista@uco.es

Dr. Rafael Carlos Estévez Toledano

Departamento Química Orgánica, Universidad de Córdoba, Campus de Rabanales, Edificio Marie Curie E-14014-Córdoba, España

Fax: (+34)957212066

E-mail: q72estor@uco.es

**Abstract**

The synthesis, by a sol-gel method, of organosilica-aluminum phosphates, (X)-AlPO(Y)-(Z), using three different silica precursors (X) 2-(4-chlorosulfonylphenyl)ethyltrimethoxysilane (C), 3-mercaptopropyl)trimethoxysilane (MPTMS) or Bis[3-(triethoxysilyl)propyl]tetrasulfide (B), with varying Al/P molar ratio (Y = 3–10) and pH of the final gel (Z = 3-9), maintaining an Al/Si= 3 molar ratio, has been carried out. Materials were characterized by XRF, SEM-EDX, XRD, $^{1}H$-$^{29}Si$ CP, $^{27}Al$ and $^{31}P$ MAS NMR and nitrogen adsorption. The acidity of the solids by TGA, XRF and XPS, as well as their catalytic behaviour in the etherification of glycerol with tert-butyl alcohol, under microwave irradiation, were evaluated. The solids with an Al/P molar ratio between 3 and 6, synthesized at a pH value over 3 with precursor C, exhibiting the highest values of acidity and predominantly a mesoporous character, showed the best catalytic behaviour.

Keywords: organosilica-aluminum phosphates; sol-gel; heterogeneous catalysts; etherification; glycerol.

## 1. Introduction

Heterogeneous solid catalysts have long been the subject of great attention due to their versatility in a huge variety of organic reactions, including biomass valorization reactions [1,2]. In fact, they are considered as one of the most important factors for the development of greener and more sustainable catalytic protocols. Recently, the possibility of including organic functionalities into an inorganic structure has also been an important step for the Heterogeneous Catalysis and Green Chemistry. Among heterogeneous solid catalysts, the acid ones containing sulfonic groups in their structure are being extensively studied, particularly in reactions that require strong Bronsted acid sites. Depending on the synthesis strategies, the properties of these sulfonic acid-based catalysts can be tailored, e.g., the pore size, the number of active sites, the hydrophobicity, etc. [1,3], making them a very versatile material.

Van Rhijn et al. [4] were pioneers in the incorporation of sulfonic acid groups over silica-based mesoporous materials. The synthesis of these materials was carried out, either by grafting (silylation or coating) of a sulfonic acid precursor, the 3-mercaptopropyltriethoxysilane (MPTMS), on the surface of an ordered silica (MCM or HMS), or by co-condensation of the precursor MPTMS with tetraethyl orthosilicate (TEOS) in the presence of a structure-directing agent. In both cases, the oxidation of the thiol group to sulfonic group was carried out with $H_2O_2$. Afterward, several methods to prepare catalysts containing sulfonic acid groups, employing different precursors, as well as different supports have been reported [4,5], though those ordered silica-based really stand out owing to their favorable characteristics, such as high specific surface area and large pore volume [4–9].

Another type of silica-based hybrid materials as the periodic mesoporous organosilicas (PMOs), that are obtained from bis-silylated organic precursors, have also

been investigated [10]. The incorporation of the sulfonic acid groups in the organic moieties of PMOs could be carried out by sulfonation of the aromatic rings [11] or of the double bonds [12], even though other approaches have been considered as the use of thioether-bridged mesoporous organosilicas containing disulfide or tetrasulfide moieties [13]. The subsequent oxidation of these bridges generates two sulfonic acid groups closely to each other.

Sulfonated carbons have also emerged as promising catalysts, since the carbons can be obtained from low-cost available biomass, making them completely renewable, and besides they can be sulfonated by a simple treatment with concentrated $H_2SO_4$. Thus, in the last years, sulfonated carbons obtained from different sources, such as glycerol [14], coffee ground [15], olive stones [16] and so on, have been reported, giving outstanding results in a wide type of organic reactions [15–18].

Ion-exchange resins and specifically, the Amberlyst-15, a macroreticular ion-exchange resin based on polystyrene-divinylbenzene modified with sulfonic groups, have also been extensively applied in organic reactions requiring a high acidity, such as esterification, etherification, etc. [18–20]. However, the main drawback for the use as catalysts of this type of ion exchange resins is the lack of thermal stability, as well as their tendency to shrink or swell in an organic medium [19].

Recently, we have reported on the synthesis of amorphous organosilica-aluminum phosphates with sulfonic groups incorporated into their structure and their behaviour catalytic in the etherification of glycerol with *tert*-butyl alcohol [21]. The incorporation of the sulfonic groups through several organosilica compounds and hence, the acidity of the materials, as well as their textural properties were all dependent on the Al/P molar ratio (from 0,5 to 1.5); the calcination temperature (250ºC and 310ºC) and the type and amount of organosilica precursor (2.5, 4 and 10 mmol) employed in the synthesis. The

results obtained in the etherification of glycerol proved that the formation of the di-tert-butyl glycerol ethers (DTBGs) and tri-tert-butyl glycerol ether (TTBG), usually called high ethers (h-GTBE), is favored over the solids exhibiting high acidity and a balanced percentage of mesopores and macropores, being the most active that solid prepared with 10 mmol of 2-(4-chlorosulfonyphenyl)ethyltrimethoxysilane, the highest Al/P molar ratio (1,5) y calcined at 250ºC. The influence of the acid and textural properties on the catalytic performance has also been verified in recent studies carried out by our research group, in which different zeolites [22] and solids based on silica [23], titania and silica-titania [24] functionalized with sulfonic acid groups were successfully employed as catalysts in the same etherification reaction.

Based on these previous results, we proposed the synthesis of similar organosilica-aluminum phosphates, but containing a greater amount of aluminum (Al/P from 3 to 10) and varying the final pH (from 3 to 9) in the synthesis in order to enhance the incorporation of sulfonic groups, through the interaction between the species of Si and of Al, and to prepare materials with tunable porosity. Furthermore, an additional organosilica precursor, containing tetrasulfide moieties, have also been employed in order to generate two sulfonic acid groups from one precursor molecule. The materials were characterized by XRF, TGA, XRD, SEM, $^{1}H$-$^{29}Si$ CP, $^{27}Al$, $^{31}P$ and $^{29}Si$ NMR MAS, and nitrogen adsorption-desorption techniques. Their catalytic activity was tested in the etherification of glycerol with *tert*-butyl alcohol that has an additional interest of producing chemical compounds of high added-value as the h-GTBE. These ethers can be employed as excellent oxygenated additives for gasoline, diesel and biodiesel, given their high oxygen content and favorable physicochemical properties, such as viscosity, flash point, cetane number, etc., providing a decrease in the emission of particulate matter, carbon oxides and carbonyl compounds in exhaust gases [25,26].

## 2. Experimental

### *2.1. Synthesis of the catalysts*

The organosilica-aluminum phosphates were prepared by a sol-gel method following the same procedure previously described by Estévez et al. [21]. Briefly, an aqueous solution of $AlCl_3 \cdot 6H_2O$ (purity ≥ 99.0%, Fluka Analytical), containing 31 mmol of Al, was kept under magnetic stirring (900 rpm) and mixed with the appropriated amount of $H_3PO_4$ (85 wt.%, PanReac AppliChem) in an ice-water bath to achieve the desired theoretical Al/P molar ratio (3, 4, 6 and 10). The resulting mixture was kept under stirring for 20 minutes and then, 10 mmoles of the sulfonic group precursor, 2-(4-Chlorosulfonylphenyl)ethyltrimethoxysilane (C) (50% solution in dichloromethane, Acros Organics) or (3-Mercaptopropyl)trimethoxysilane (MPTMS) (95%, Alfa Aesar) or Bis[3-(triethoxysilyl)propyl]tetrasulfide (B) (≥ 90%, Sigma-Aldrich), were added dropwise. After 15-20 minutes, aqueous ammonia ($NH_4OH$ 25%, Panreac AppliChem), was slowly added until the desired pH (3, 5, 7 and 9) was adjusted. The final synthesis gel was then kept at room temperature for 24 h. The solid obtained was filtered off, washed with isopropyl alcohol (≥ 99.8%, Sigma-Aldrich), and dried at 120° C for 24 h. Then, the solids were powder screened to <0.149 mm and calcined at the required temperature in air for 3 h. The catalysts were denoted as X-AlPO(Y)-Z where X is the organosilica precursor; Y the Al/P molar ratio; and Z is the final pH of the gel. The solids prepared from C were calcined at 250 °C, whereas those prepared either from B or MPTMS were calcined at 210 °C due to the lower thermal stability of these groups in comparison with the arenesulfonic ones. The solids prepared either from the sulfonic group precursors B or MPTMS were treated with $H_2O_2$ (33% w/v, 110 vol. stabilisiert, PanReac AppliChem) after calcination, in order to oxidize either the tetrasulfide bridges (S-S-S-S) or the thiol group (–SH) to sulfonic groups (-

$SO_3H$), in accordance with a previously described procedure [23]. Thus, 0.3 g of each solid was treated with 40 mL of $H_2O_2$ (30% v/v) in a round bottom flask with magnetic stirring for 3 hours. The round bottom flask was placed in a thermally controlled oil bath at 50 °C. The solid obtained was filtered off and washed with ethanol twice. Once the process is finished, the solids were dried in a conventional oven at 120 °C. All the solids were powder screened to <0.149 mm to avoid internal diffusion limitations in the reactions.

(Scheme 1 near here)

As a reference, a solid (Si-Al) with Si (from C precursor) and Al, but without P, was also obtained and calcined in the same way as has been described for the organosilica-aluminum phosphates. In this case, the final pH was 5.

*2.2.Characterization of the catalysts*

The P, Al, Si and S content in the solids was determined by X-ray fluorescence measurements on a ZSX primus IV instrument from Rigaku, using the fundamental parameters in a semi- quantitative analysis. The final amount is the average of two measurements being the estimated error ≤ 6%.

The morphology and surface composition of the solids were analyzed using Scanning Electron Microscopy–Energy Dispersive X-ray spectroscopy (SEM-EDX). Scanning electron micrographs and energy-dispersive spectra were acquired with a JEOL JSM 7800F microscope. The measurements were repeated at least three times on different zones of the material surface (experimental error ≤ 4%).

XRD patterns were obtained using a Discover (Bruker) diffractometer equipped with Cu Kα monochrome radiation (λ=1.5406Å). Finely ground samples were scanned at a speed of 2º/min (2°≤ 2θ ≤ 70°).

Textural properties were determined from the $N_2$ adsorption-desorption isotherms at - 196 ºC using a Micromeritics ASAP 2010 apparatus. Prior to measurements, all the samples were degassed at 120 ºC for 12 h. The specific surface area of each solid, $S_{BET}$, was determined by using the Brunauer–Emmett–Teller (BET) method at relative pressures in the range $p/p_0$ = 0.05-0.3 assuming a cross-sectional area of 0.162 $nm^2$ for the nitrogen molecule. The values of pore volume and the pore size distributions were calculated by the Barret-Joyner-Halenda (BJH) method, assuming a cylindrical pore model.

Thermogravimetric analysis (TGA) was recorded on a TGA/DSC 1 Star System Mettlet Toledo thermal analysis station by heating under an $O_2$ flow of 100 mL/min from 30 °C to 700 °C at a rate of 10 °C/min. An alumina sample holder with capacity of 70 μL was employed.

All NMR spectra were recorded at a Bruker spectrometer, model AVANCE III HD of 400 MHz, equipped with a rotor of 3.2 mm. $^{1}H$-$^{29}Si$ CP MAS NMR spectra were acquired at a resonance frequency of 79.4 MHz, with a spinning speed of 10 KHz, using a 7 ms pulse, a 5 s repetition time, and 15000 scans. $^{29}Si$ MAS NMR spectra (30º simple pulse) were performed at 79.4 MHz, with a spinning speed of 10 KHz, using a 100 s repetition time, and 2000 scans. $^{27}Al$ NMR spectra (10º simple pulse) were obtained at 104.2 MHz, with a spinning speed of 13 KHz, using a 0.3 s repetition time, and 10000 scans. $^{31}P$ NMR spectra (90º simple pulse) were obtained at 161.3 MHz, with a spinning speed of 13 KHz, using an 80 s repetition time, and 600 scans. Tetramethylsilane (TMS) was used as external standard reference for $^{29}Si$ chemical shifts, while $^{27}Al$ and $^{31}P$ were referenced to an aqueous solution of $Al(NO_3)_2$ (1 M) and $H_3PO_4$, respectively.

XPS spectra were recorded with a SPECS Phoibos HAS 3500 150 MCD, under the residual pressure in the analysis chamber of $5x10^{-9}$ Pa. Accurate binding energies were

determined with respect to the position of the Si 2p peak at 103.4 eV. The peaks were decomposed using a least-squares fitting routine (Casa XPS software) with a Gaussian-Lorentzian (70:30) using Shirley baselines.

*2.3. Etherification of glycerol*

Microwave-assisted etherification of glycerol (≥99.5%, Sigma-Aldrich) with *tert*-butyl alcohol (≥ 99.7%, HoneyWell) was carried out in a CEM-DISCOVER apparatus with PC, at the reaction conditions described elsewhere [21]. In a typical run, the composition of the reaction mixture was: 0.4 g of glycerol, TBA/G molar ratio of 4 and constant catalyst loading of 5 wt.% (referred to initial glycerol mass). The total volume of the reactant mixture was 2 mL and the reaction temperature of 85 ºC. After 15 min of reaction, the sample was cooled down in an ice bath, filtered off and subsequently analyzed. Blank experiments showed that the mixture of TBA/G did not react in the absence of catalyst at the experimental conditions employed. Also, not diisobutylene (DIB) or secondary products coming from glycerol were obtained under these conditions.

Samples were analyzed by GC in a Hewlett Packard 5890 series II, equipped with a Supelcowax 10 capillary column (100% ethylene glycol 30m x0.25 mm x0.25μm), and a FID detector, using 4-chlorotoluene (≥ 99.0%, Fluka) as an internal standard [21,24]. The analysis program was: 60 °C for 6 min heating at 20 °C/min until 240 °C with an analysis time of 25 min. The conversion of glycerol ($X_G$) and product selectivity (S) were determined by the following equation:

$$X_G\ (\%) = \frac{\text{mmol of products}}{\text{starting mmol of G}} \times 100 \qquad \text{(Equation 1)}$$

$$S_i\ (\%) = \frac{\text{mmol of compound i}}{\text{mmol of products}} \times 100 \qquad \text{(Equation 2)}$$

Site Time Yield (STY) was calculated as mmol of produced h-GTBE per mmol of active specie $SO_3H$ (calculated from TGA) per hour. In order to study the reusability of the solids under the same reaction conditions, the catalyst was recovered at the end of the reaction, washed with ethanol (99.5%, PanReac AppliChem) and dried at 100ºC. Afterwards, it was tested again following the above-mentioned procedure.

## 3. Results and discussion

### 3.1. *Chemical composition of the solids*

In general, the experimental Al/P molar ratio values from XRF, Table 1, were higher than the theoretical ones, which would indicate that not all phosphorus had precipitated and was eliminated as phosphate ions in the washing solutions (≤ 25% mol), being this loss especially remarkable in C-AlPO(3)-5 and C-AlPO(4)-5. In addition, the amount of Si (mmol/g) incorporated is in the range from 0.5 to 1.6 mmol Si/g, being the C-AlPO(3)-5 which incorporated the highest amount, corresponding to the 92% in relation to the initial amount of silicon added during the synthesis procedure. This value was higher than that obtained in previous studies for the organosilica-aluminum phosphates synthesized with an Al/P molar ratio equal or less than 1.5 at a pH=5 with the same precursor, which was around 50-60% [21].

As expected, the amount of Si and S in all the C-AlPO(Y)-Z solids were very similar, considering the chemical composition of C precursor. However, in the solids synthesized from MPTMS and B precursors the amount of S incorporated was slightly lower than that of silicon (Table 1). This fact could be related to the rupture of some C-Si bonds in the oxidation reaction of the thiol groups or of the tetrasulfide bridges into sulfonic acid groups. The results obtained in the $^{1}H$–$^{29}Si$ CP MAS NMR confirmed such rupture (see below).

With regard to the superficial composition of the catalysts as seen in the SEM-EDX results (Table 1), an enrichment of Al in the surface was generally observed, since the Al/P molar ratio was slightly superior (<10%) to that obtained by XRF measurements (bulk composition).

(Table 1, near here)

### 3.2. *Textural Properties*

Adsorption-desorption nitrogen isotherms and the pore size distribution of the solids are depicted in Figure S1. In general, the most of solids exhibited type IV isotherms with a step at a relative pressure around 0.6-0.9, typical of solids with pores in a high mesoporous range, exhibiting a wide pore size distribution as well, with values ranging between 7 and 40 nm. However, some of the synthesized catalysts, such as the C-AlPO(10)-5, Figure S1A (d), and the C-AlPO(4)-3, Figure S1B (a), catalysts exhibited a type II isotherm, characteristic of macroporous materials.

Table 1 compiles the BET surface area and pore volume values for all the synthesized catalysts. As can be seen, the $S_{BET}$ values decreased as the amount of Al increased, attaining a non-porous solid with the highest Al/P molar ratio of 10, Table 1 and Figure S1A. This fact has been previously observed when different metals, i.e., iron [27] or vanadium [28], were incorporated in an aluminum phosphate system. In addition, the presence of phosphorus seemed to favor the obtention of solids with high surface area, since the reference solid, the Al-Si material, exhibited a lower $S_{BET}$ value than its counterpart synthesized with phosphorus, the C-AlPO(3)-5 (25 and 93 $m^2/g$, respectively). Accordingly, solids with Al/P molar ratio of 3 or 4 exhibited mainly a mesoporous character (~80% of mesopores, Table 1). However, a further increase in the aluminum content promoted the formation of macropores, reaching almost a 100% of macroporosity when the Al/P molar ratio is 10.

The final pH in the gel seems to be a critical factor in obtaining a material with adequate textural properties, depending on of type of reaction in which it will be applied. As can be seen in Table 1, a very acid final pH gave rise a catalyst, C-AlPO(4)-3, with the lowest surface area (3 $m^2/g$) and macroporous character (Table 1, entry 5). As the pH increased, the $S_{BET}$ of the solids, as well as their mesoporous character also increased. In fact, the solid synthesized at pH of 9, C-AlPO(4)-9, exhibited the highest surface area, 190 $m^2/g$, and the highest percentage of mesoporous as well, 97% (Table 1, entry 7).

The organosilica precursor employed (Figure S1C) did not induce important changes in the mesoporous character of the solids, although when the di-silane precursor (B) was employed, a material with a higher $S_{BET}$ (119 $m^2/g$) than that exhibited by their counterparts C (82 $m^2/g$) or MPTMS 82 (76 $m^2/g$) was obtained (Table 1, entries 2, 8 and 9). Furthermore, a slightly higher pore size was exhibited by the solid containing the MPTMS precursor (34 nm) in comparison with C and B precursors, which showed a pore diameter of 17 and 10 nm, respectively.

*3.3. Structural Characterization*

The XRD patterns of the solids (Figure S2) showed a broad band in the range of 10-30° (2θ), characteristic of the amorphous metal phosphates and silica. This fact indicated that changes in the studied synthesis parameters, i.e., Al/P molar ratio, the final pH of synthesis and the organosilica precursor, did not induce crystallinity in the morphology of the solids. The amorphous character of all the solids was also verified by SEM, as shown in the Figure 1(a), for C-AlPO(4)-9 solid. This micrograph, and the rest of them (not shown here) revealed a very widely varied distribution in morphology, texture and particle sizes. Mainly, two types of particles were observed. The first one, similar to that on the left of the image, is typical of the amorphous aluminum phosphate

[27], as can be corroborated by the mapping images (Figure 1(b)). The second one, that exhibits a spherical-like shape (center of the image), seems to be growing up from the aluminum phosphate particle. This particle contains a higher proportion of silicon and sulfur than the first one, although aluminum and phosphorus are also present.

(Figure 1, near here)

The incorporation of the siloxane to the structure as well as the interaction between Si with itself, with Al and/or with P have been studied by $^{1}$H-$^{29}$Si CP MAS NMR, $^{29}$Si, $^{27}$Al and $^{31}$P NMR spectroscopy.

As can be seen in the Figure 2, all the $^{1}$H–$^{29}$Si CP MAS NMR spectra displayed a broad feature extending from -45 ppm to –80 ppm with a maximum around –67 ppm and two shoulders around -57 ppm and –47 ppm. In theory, these signals can be assigned to R-Si(OSi)$_3$ ($T^3$), R-Si(OSi)$_2$(OH) ($T^2$), and R-Si(OSi)(OH)$_2$ ($T^1$) species, respectively [8,29]. From deconvoluted spectra, the specific isotropic chemical shift values, as well as the integrated intensity for each peak were obtained (Table 2). For the solid with Al/P=3 the $T^3$ were the main species (86%), while as the Al/P ratio increased, the $T^3$ species diminished at the expense of increasing the $T^2 + T^1$ species, so that the solid with Al/P = 10 exhibited a $T^2 + T^1$ superior to 50%. Likewise, a higher percentage of $T^2 + T^1$ (54%) than $T^3$ is found in the solid synthesized at pH= 3, C-AlPO(4)-3, and in that obtained from B precursor, B-AlPO(4)-5, (58%). Based on the value of isotropic chemical shift, it is difficult to know the silicon environments, since the values for R-Si-O-Al is found in the same range as that for R-Si-OH [21,30]. However, at least one Si atom in $T^3$ species, but more of one in $T^2$ and $T^1$ might be bonded to Al and P, being more probable the Al, since the P-O-Si bond has high tendency to be hydrolyzed in the present hydrolytic conditions [30]. In fact, there was no bands in the range from -112 to -214 ppm, typical of this linkage [31]. In addition, the existence of R-

$Si(OSi)(OAl)_m(OH)_{2-m}$ (m=1-2) species in the synthesized solids can be confirmed by two facts. The first one, the incorporation of the organosiloxane in the reference solid (Si-Al) (Table 1). The second one, the verification that the ratio of the intensity of the species $T^2+T^1/ T^3$ in both the $^1H–^{29}Si$ CP MAS NMR and the $^{29}Si$ MAS NMR spectra, remained constant in the majority of the solids (Figure 2, dotted red lines). Consequently, the increase in the intensity of the signals in the $^1H–^{29}Si$ cross polarization MAS NMR spectra ought to be due mainly to the coupling of the Si nucleus with the hydrogen atoms of the organic radical. Moreover, the resonances corresponding to $T^1$ and $T^2$ shifted toward lower field, especially for the solids containing an Al/P molar ratio $\geq$ 4, which is accordance with the value of −47 ppm reported for $(MeSi(OAl)_3$ groups [32]. Hence, the silicon should be surrounded by aluminum rather than by –OH groups. However, an exception was found in the solid C-AlPO(10)-5, since the $T^1+T^2/T^3$ ratio was slightly higher in the cross-polarization spectrum, indicating a greater presence of –OH groups linked to Si (R-SiOH units) (Figure 2A(d)).

(Table 2, near here)

It is worth indicating the presence of some signals between -80 and -120 ppm assigned to $Q^n$ structures, $Si-(OSi)_n(OH)_{4-n}$ (n= 2-4) or $Si-(OSi)_n(OAl)_{4-n}$ (n= 1–3) [8,30,33] in the spectra of MPTMS-AlPO(4)-5 and B-AlPO(4)-5. These $Q^n$ signals can be ascribed to the rupture of some C-Si bonds of the precursor, mainly due to the acid medium and/or the oxidation treatment necessary to transform the thiol group (-SH) or the tetrasulfide bridge (S-S-S-S) in sulfonic groups ($-SO_3H$). In fact, the materials MPTMS-AlPO(4)-5 and B-AlPO(4)-5, which were subjected to oxidation treatments, showed the highest proportion of $Q^n$ signals, around 13 and 22%, respectively (Figures 2C, (b-c)). Analogously to what happened with the $T^m$ signals, when comparing the $^1H-^{29}Si$ CP MAS NMR with $^{29}Si$ MAS NMR, the intensity of those $Q^n$ signals should

increase for effect of the OH groups bond to Si atoms. As can be seen in Figure 2C, these $Q^n$ signals were very similar for B-AlPO(4)-5 (Figure 2C(c)) in both type of spectra, whereas in the case of the MPTMS-AlPO(4)-5 solid, an increment in the majority of the $Q^n$ signals in the $^{1}H$-$^{29}Si$ CP NMR spectrum was observed (Figure 2C(b)).

The $^{27}Al$ NMR spectra of the solids are collected in Figure 3. Three well-defined signals can be observed in majority of them. The first one, at +39-43 ppm, which is a typical resonance of Al sharing oxygen atoms with four tetrahedra of P, the second one, at +14-19 ppm, is associated to penta-coordinated aluminum and the third one, between -10 and -14 ppm, is usually assigned to octahedral aluminum partially coordinated with hydroxyl groups [34]. Particularly, the C-AlPO(3)-5 solid exhibited these three resonances, but at lower field, i.e., +64.3, +35.0 and -2.4 ppm (Figure 3A(a)). According to literature [30,33], this change can be due to the existence of Si atoms in the second coordination sphere of Al. In fact, a peak in the range of +55 to +70 ppm is characteristic of an $Al(OSi)_4$ tetrahedral. Hence, in the solid that incorporated the highest amount of silicon in its structure (92.2%, Table 1) the aluminum sites regardless of their coordination number, exhibited a clear interaction with neighbor silicon atoms. However, the existence of Al atoms in the second coordination sphere cannot be ruled out either. Thus, C-AlPO(10)-5 and the Si-Al reference solid, both with the highest Al content exhibited values of chemical shifts at lower field, +75 ppm, +40 ppm and +6-7 ppm, that are similar to the resonances of Al sites lying in four-, five- and six-coordination in an alumina [35,36]. Therefore, in the solids with the greatest amount of Al (solid with Al/P molar ratio=10 and reference solid) the interaction of Al with itself, rather than with Si is favored.

Regarding the $^{31}$P NMR (Figure S3), all the solids exhibited similar spectra with one broad and mostly symmetrical signal, regardless of the synthesis parameters employed. In the majority of the cases, the deconvolution of this signal gave rise two components. The minor component (7-39%), with a chemical shift value between -23 and -28 ppm, is typical of tetrahedrally coordinated phosphorous in amorphous aluminum phosphates [21,37], while the major component (51-100%) appeared at lower field, between -15 and -19 ppm, that could be assigned to phosphorous linked to high-coordinated (penta- or hexa-coordinated) Al atoms [36,38,39]. This assignment would be in accordance with the results from $^{27}$Al RMN, indicating the predominance of the Al sites in octahedral coordination. Furthermore, the changes in the percentage of octahedral Al and in the percentage of P linked to these type of Al sites followed the same tendency, in function of the composition of the solids and the final pH (Table 2).

Taking into account the results obtained in the analysis of the solids by $^{29}$Si, $^{27}$Al and $^{31}$P MAS NMR, as well as their bulk and superficial composition, we can assume that in the solids C-AlPO(Y)-Z, with Al/P < 10 and final pH = 5, domains of Si cross-linked polymeric structures dispersed in a disordered aluminum phosphate mainly exist. The Al is preferably in octahedral coordination, being the domains linked by interface Si-O-Al bonds. The Si structures became less compact as the P content decreased, Al/P= 4 and 6. When the P content in the solid is very low (Al/P=10), domains of alumina and of Si oligomeric structures forming linear chains with little cross-linked, seems to exist. The final pH did not seem to have a great influence on the structure of the solids, existing cross-linked polymeric structures of Si dispersed in a disordered aluminum phosphate, as well as Si oligomeric structures growing from alumina domains, as indicated in Figure 1. The solid prepared with MPTMS precursor presents a similar structure to that prepared with C precursor, showing both the same percentage of

Si incorporated. On the contrary, in the solid prepared with B precursor the Si oligomeric chains were dominant.

(Figures 2 and 3, near here)

*3.4. Acidity of the synthesized solids*

The acidity of the solids (mmol S/g) can be calculated from the amount of sulfur obtained by XRF and the percentage of oxidized sulfur obtained by XPS (Table 1, Figure S4). In the case of C-AlPO(Y)-Z solids, the sulfur is all in sulfonic form, so the acidity matches with the amount of sulfur obtained from XRF. Therefore, the higher the amount of sulfur incorporated, the higher the acidity value of the solid.

Thermogravimetric analyses (TGA) were performed to ascertain the thermal stability of the catalysts as well as to confirm the introduction of both, the thiol groups and the sulfonic acid groups. As it can be seen in Figure 5, three weight losses up to 600 ºC were mainly observed on all the X-AlPO(Y)-Z solids. The first weight loss (4-12%), under 200 ºC, can be attributed to the removal of physisorbed water and the isopropyl alcohol employed during the synthesis procedure, while the second one, up to 310 ºC, can be ascribed to the removal of ammonium chloride (3-7%), as was previously reported for aluminum phosphate system [21,28]. Finally, the third weight loss, observed between 350 and 600 ºC, has been related in the literature to the loss of organosulfonic acid groups [8,14,40].

(Figure 4 near here)

Figure 4(a) shows the TG profiles of the solids synthesized with different Al/P molar ratios. As can be seen, the greatest weight loss (around 24%) in the range 350-600ºC was obtained for C-AlPO(3)-5 and C-AlPO(4)-3 materials, whereas the rest of them exhibited similar weight losses at this range of temperature (around 19%). About the organosilica precursors, Figure 4(b), the solid with the precursor C showed the

greatest weight loss (19%), followed by the MPTMS-AlPO(4)-5 (12%) and B-AlPO(4)-5 (6%). Last but not least, the TGA of the solids synthesized at different pH are depicted in Figure 4(c). The weight losses observed are very similar independently on the pH of the final gel. In fact, the highest weight loss was exhibited by the solid synthesized at a pH of 3 (25%), whereas the weight loss observed for the solids synthesized at a pH of 5, 7 and 9 were similar, 19, 22 and 20%, respectively.

The TGA results allow us to quantify the amount of sulfonic groups in the solids, since it can be calculated from the weight loss obtained in the range 350-600 ºC, for the case of solids containing the precursor C and in the range 300-550 ºC for the solids synthesized, either with the precursor MPTMS or B. The decrease in the final temperature was due to the lower thermal stability of these groups in comparison to the arenesulfonic ones. The quantity of sulfonic groups obtained by TGA can be directly related with the acidity, as mmol $SO_3H$/g of catalyst (Table 1). As can be seen, for the C-AlPO(X)-Y solids, the highest value (1.3 mmol $SO_3H$/g) was exhibited by the C-AlPO(3)-5 and C-AlPO(4)-3 solids. Identical value of acidity displayed the reference solid (Si-Al). On the contrary, the solid with the lowest acidity value was the B-AlPO(4)-5 (0.5 mmol $SO_3H$/g). In general, the values of acidity determined from TG measurements followed the same tendency as the silicon incorporation measured by XRF.

The XPS analyses were performed to ascertain and quantify the percentage of oxidized sulfur in MPTMS-AlPO(4)-5 and B-AlPO(4)-5 cases. In the XPS spectra (Figure S4), the peak around 169 eV is attributed to sulfur in sulfonic form (-$SO_3H$) while the peak around 163 eV is characteristic of sulfur in thiol form (-SH), with an oxidation state of +2, Figure S4(a-b). After the oxidation treatment, the 80% of the thiol groups in the MPTMS-AlPO(4)-5 were oxidized to sulfonic groups, whereas the 100%

of the sulfur was oxidized to sulfonic groups in the case of B-AlPO(4)-5 material, Figure S4(d-e).

*3.5. Etherification of glycerol*

The well-known reaction mechanism of the etherification of glycerol with tert-butyl alcohol is described in Figure S5. Briefly, a fast protonation of TBA on acid sites occurs, giving rise to a tertiary carbocation that reacts with glycerol, generating MTBGs. Sequentially, MTBGs react with TBA to form the DTBGs, which react again with TBA to achieve TTBG. Additionally, during the process, water is produced as a by-product [41,42]. It is important to notice that in the present study, a small amount of isobutylene (IB) < 6%, coming from the dehydration of the TBA, was also obtained.

Table 3 shows the catalytic performance of the solids studied in the microwave-assisted etherification reaction of glycerol with tert-butyl alcohol after 15 min of reaction time. As can be seen, the majority of C-AlPO(Y)-Z catalysts exhibited similar behavior in the etherification reaction with values of glycerol conversion over 55% and of selectivity to h-GTBE around 20%, mainly those obtained with an Al/P molar between 3 and 6 and a pH of the final gel over 3. This result was expected given the similar acidity values that these catalysts exhibited (between 1 and 1.3 mmol $SO_3H$/g from TGA measurements). However, the C-AlPO(10)-5 and C-AlPO(4)-3 displayed a much lower values of conversion (19 and 14%, respectively) and of selectivity to h-GTBE (9%) than their C-AlPO counterparts, despite they exhibited acidities in the range of all the C-AlPO catalysts (1.1 mmol $SO_3H$/g for C-AlPO(10)-5 and 1.3 mmol $SO_3H$/g for C-AlPO(4)-3). Therefore, another factor in addition to the acidity should influence the catalytic performance. To explain this behavior, the catalytic performance was also related to the textural properties of the materials. C-AlPO(10)-5 and C-

AlPO(4)-3 catalysts exhibited a non-porous character with the lowest surface area values among all the C-AlPO catalysts (3 $m^2/g$). This entails a high density of acid sites, which could favor the hydrolysis reactions of the ethers formed, and consequently, the equilibrium of the reaction would be reached long before than with the catalysts with a lower density of acid sites. In fact, considering the STY value, where the active sites exhibited by the catalysts and the time employed are taken into account, it must be said that the value obtained on non-porous catalysts was of the order of 10 times lower than for the rest of the C-AlPO(Y)-Z, Table 3. Therefore, catalysts with a high surface area would allow a better dispersion of the sulfonic acid sites. In addition, the high pore volume of these catalysts would allow a good diffusion of the molecules through the pores, promoting the molecules contact with the active sites of the catalyst. The behavior of the reference solid, Si-Al, can be also explained on based in its textural properties. These results corroborate those previously obtained by our Research Group employing sulfonic acid silica- or titania-based catalysts [24], where a combined effect of acidity and textural properties was necessary for a good performance of the catalyst.

Regarding the MPTMS-AlPO(4)-5 catalyst, a lower glycerol conversion (28%) than its counterpart synthesized with precursor C (55%) was obtained. This fact can be ascribed to the lower acid strength of propyl-$SO_3H$ sites of MPTMS in comparison to that of arene-$SO_3H$ moieties, as it is well-known, in clear accordance with results previously reported [8,21]. Nevertheless, no significant differences were observed in terms of selectivity, since textural properties of C-AlPO(4)-5 and MPTMS-AlPO(4)-5 are similar. The inferior results obtained on B-AlPO(4)-5 ($X_G$ = 18% and $S_{h\text{-}GTBE}$ = 8%) can be explained firstly by its less acidity (0.5 mmol $SO_3H/g$) and secondly, by the character of the sulfonic groups (propyl-$SO_3H$) presented in the solid.

(Table 3, near here)

Based on the present results, one more solid was synthesized with precursor C in order to join the most favorable characteristics for the reaction to be performed. These synthesis conditions were Al/P molar ratio of 6, because it is the highest Al/P molar ratio before a high amount of alumina is formed, and pH of 6, to obtain a good balance between surface area and mesoporosity. The C-AlPO(6)-6 exhibited a surface area of 70 $m^2/g$ with a 90% of mesoporous character, a pore volume of 0.38 $m^3/g$, as well as the highest acidity value (1.4 mmol $H^+/g$) measured by TGA, as is shown in Table 1. This catalyst exhibited the highest glycerol conversion value (97%), Table 3, with a $S_{h\text{-}GTBE}$ equal to those obtained with the more actives C-AlPO catalysts. Therefore, we can highlight the versatility of the synthesis procedure in order to obtain catalysts with interesting physicochemical and acidic properties, depending on the reaction in which they will be applied.

3.6. *Reusability and Catalyst Stability*

The stability of some of the solids was studied during different cycles of glycerol etherification, Table 4. As can be seen, all the catalysts tested maintained their activity after the first cycle. In addition, the stability of the C-AlPO(6)-6 was study up to the $4^{th}$ use. As shown, the yield to h-GTBE decreased after the second use (from 16% to 10%), keeping constant after the $3^{rd}$ cycle. Then, after the $4^{th}$ cycle of the reaction, the yield to h-GTBE decreased again up to 4%. This behavior has been previously observed over organosilica-aluminum phosphates previously synthesized [21] by the same procedure. In that case, the loss of activity was associated with a poisoning of the catalyst from organic molecules that could have remained adsorbed on the solid after the reaction [9,24]. To corroborate this, the spent catalysts was subjected to a previous procedure consisting in an extraction with ethanol under reflux for 3 h. Then, the solids were dried, and the liquid fraction was distilled to eliminate the solvent ethanol. The organic

fraction was then analyzed by GC, and glycerol and other products of the reaction (mainly MTBGs and DTBGs) were found. Then, the cleaned catalyst was tested again, observing that the catalytic activity was recovered.

(Table 4, near here)

**Conclusion**

In summary, a good incorporation of Si and S was obtained in the organosilica-aluminum phosphates obtained at values of Al/P molar ratio from 3 to 6 and a pH of 5. The choice of compound C as organosilica precursor against thiol group (MPTMS) and tetrasulfide bridge (B) is confirmed with the best results here obtained, since the oxidation treatment needed to obtain sulfonic groups, when MPTMS and B precursors are employed, promoted the rupture of some C-Si bonds, diminishing the incorporation of sulfur respect to the silicon. An enrichment of Al in the catalysts surface was observed, whereas phosphorus did not precipitate in its entirety, being eliminated as phosphate ions in the washing solutions (≤ 25% mol). Nevertheless, the aluminium phosphate structure, although disordered, seem to be crucial for both, the Si incorporation and textural properties of the solids. The Al/P molar ratio and the final pH in the gel seem to be critical factors in obtaining solids with a higher Si incorporation and adequate textural properties, being the optimal values of Al/P between 3 and 6, as well as pH over 3. It can be assumed that the structure of those solids consists of domains of Si cross-linked polymeric structures dispersed in a disordered aluminum phosphate. As the P decreased (Al/P = 10), domains of alumina and Si oligomeric structures with little cross-linked seems to be formed. The acidity of the solids is totally related to the sulfur amount.

The differences in the catalytic activity of the solids in microwave-assisted etherification of glycerol with *tert*-butyl alcohol at 85 °C and at autogenous pressure,

ought to be explained by both, acidity and textural properties. Hence, catalysts with a high acidity and mesoporous character exhibited the best catalytic results ($Y_{h\text{-}GTBE} \geq$ 11%). Thus, a good dispersion of the sulfonic acid sites seems to be essential in order to avoid the hydrolysis of the ether bonds formed and, therefore, preventing equilibrium from being reached prematurely. Additionally, the stability of the solids has been demonstrated after several reuses.

From the present results, we can open new perspectives on the design and synthesis of efficient catalysts based on organosilica-aluminumphosphates, for reactions that require strong Bronsted acid centers, such as the reaction here studied.

**Acknowledgments**

The authors are grateful for the funding received from Spanish MICINN through the project PID2019-104953RB-I00, the Junta de Andalucía and FEDER (P18-RT-4822) and the UCO-FEDER (1264113-R). The technical support and facilities from Cordoba University´s SCAI are greatly appreciated. L. Aguado-Deblas and R. Estevez are indebted to the Junta de Andalucia for the contract associated to P18-RT-4822 Project.

## References


[1] P. Sudarsanam, E. Peeters, E. V. Makshina, V.I. Parvulescu, B.F. Sels, Advances in porous and nanoscale catalysts for viable biomass conversion, Chem. Soc. Rev. 48 (2019) 2366–2421.

[2] Y.M. Sani, W.M.A.W. Daud, A.R. Abdul Aziz, Activity of solid acid catalysts for biodiesel production: A critical review, Appl. Catal. A Gen. 470 (2014) 140–161.

[3] E. Doustkhah, J. Lin, S. Rostamnia, C. Len, R. Luque, X. Luo, Y. Bando, K.C.W. Wu, J. Kim, Y. Yamauchi, Y. Ide, Development of Sulfonic-Acid-Functionalized Mesoporous Materials: Synthesis and Catalytic Applications, Chem. - A Eur. J. 25 (2019) 1614–1635.

[4] W.M. Van Rhijn, D.E. De Vos, B.F. Sels, W.D. Bossaert, P.A. Jacobs, Sulfonic acid functionalised ordered mesoporous materials as catalysts for condensation and esterification reactions, Chem. Commun. (1998) 317–318.

[5] J.A. Melero, R. van Grieken, G. Morales, Advances in the synthesis and catalytic applications of organosulfonic-functionalized mesostructured materials, Chem. Rev. 106 (2006) 3790–3812.

[6] L.L. Owen, R. W., Gestwicki, J. E., Young, T., and Kiessling, Synthesis and Applications of, Org. Lett. 4 (2002) 2293–2296.

[7] D. Margolese, J.A. Melero, S.C. Christiansen, B.F. Chmelka, G.D. Stucky, Direct syntheses of ordered SBA-15 mesoporous silica containing sulfonic acid groups, Chem. Mater. 12 (2000) 2448–2459.

[8] J.A. Melero, G.D. Stucky, R. van Grieken, G. Morales, Direct syntheses of ordered SBA-15 mesoporous materials containing arenesulfonic acid groups, J. Mater. Chem. 12 (2002) 1664–1670.

[9] S. Kaiprommarat, S. Kongparakul, P. Reubroycharoen, G. Guan, C. Samart,

Highly efficient sulfonic MCM-41 catalyst for furfural production: Furan-based biofuel agent, Fuel. 174 (2016) 189–196.

[10] F. Hoffmann, M. Cornelius, J. Morell, M. Fröba, Silica-based mesoporous organic-inorganic hybrid materials, Angew. Chemie - Int. Ed. 45 (2006) 3216–3251.

[11] A. Karam, J.C. Alonso, T.I. Gerganova, P. Ferreira, N. Bion, J. Barrault, F. Jérôme, Sulfonic acid functionalized crystal-like mesoporous benzene-silica as a remarkable water-tolerant catalyst, Chem. Commun. (2009) 7000–7002.

[12] D. Esquivel, E. De Canck, C. Jiménez-Sanchidrián, P. Van Der Voort, F.J. Romero-Salguero, Formation and functionalization of surface Diels-Alder adducts on ethenylene-bridged periodic mesoporous organosilica, J. Mater. Chem. 21 (2011) 10990–10998.

[13] M.I. López, D. Esquivel, C. Jiménez-Sanchidrián, F.J. Romero-Salguero, Application of Sulfonic Acid Functionalised Hybrid Silicas Obtained by Oxidative Cleavage of Tetrasulfide Bridges as Catalysts in Esterification Reactions, ChemCatChem. 5 (2013) 1002–1010.

[14] M.D. González, Y. Cesteros, J. Llorca, P. Salagre, Boosted selectivity toward high glycerol tertiary butyl ethers by microwave-assisted sulfonic acid-functionalization of SBA-15 and beta zeolite, J. Catal. 290 (2012) 202–209.

[15] M. Gonçalves, F.C. Soler, N. Isoda, W.A. Carvalho, D. Mandelli, J. Sepúlveda, Glycerol conversion into value-added products in presence of a green recyclable catalyst: Acid black carbon obtained from coffee ground wastes, J. Taiwan Inst. Chem. Eng. 60 (2016) 294–301.

[16] R. Estevez, L. Aguado-Deblas, V. Montes, A. Caballero, F.M. Bautista, Sulfonated carbons from olive stones as catalysts in the microwave-assisted etherification of glycerol with tert-butyl alcohol, Mol. Catal. 488 (2020) 110921-110928.

[17] S. Kang, J. Ye, J. Chang, Recent Advances in Carbon-Based Sulfonated Catalyst:\rPreparation and Application, Int. Rev. Chem. Eng. 5 (2013) 133–144.

[18] V.L.C. Gonçalves, B.P. Pinto, J.C. Silva, C.J.A. Mota, Acetylation of glycerol catalyzed by different solid acids, Catal. Today. 133–135 (2008) 673–677.

[19] I. Dosuna-Rodríguez, E.M. Gaigneaux, Glycerol acetylation catalysed by ion exchange resins, Catal. Today. 195 (2012) 14–21.

[20] M.A. Harmer, Q. Sun, Solid acid catalysis using ion-exchange resins, Appl. Catal. A Gen. 221 (2001) 45–62.

[21] R. Estevez, S. Lopez-Pedrajas, D. Luna, F.M. Bautista, Microwave-assisted etherification of glycerol with tert-butyl alcohol over amorphous organosilica-aluminum phosphates, Appl. Catal. B Environ. 213 (2017) 42–52.

[22] R. Estevez, I. Iglesias, D. Luna, F.M. Bautista, Sulfonic acid functionalization of different zeolites and their use as catalysts in the microwave-assisted etherification of glycerol with tert-butyl alcohol, Molecules. 22 (2017) 2206-2217.

[23] R. Estevez, M.I. López, C. Jiménez-Sanchidrián, D. Luna, F.J. Romero-Salguero, F.M. Bautista, Etherification of glycerol with tert-butyl alcohol over sulfonated hybrid silicas, Appl. Catal. A Gen. 526 (2016) 155–163.

[24] L. Aguado-Deblas, R. Estevez, M. Russo, V. La Parola, F.M. Bautista, M.L. Testa, Microwave-assisted glycerol etherification over sulfonic acid catalysts, Materials (Basel). 13 (2020) 1–16.

[25] C. Beatrice, G. Di Blasio, C. Guido, C. Cannilla, G. Bonura, F. Frusteri, Mixture of glycerol ethers as diesel bio-derivable oxy-fuel: Impact on combustion and emissions of an automotive engine combustion system, Appl. Energy. 132 (2014) 236–247.

[26] A. Cornejo, I. Barrio, M. Campoy, J. Lázaro, B. Navarrete, Oxygenated fuel additives from glycerol valorization. Main production pathways and effects on fuel properties and engine performance: A critical review, Renew. Sustain. Energy Rev. 79 (2017) 1400–1413.

[27] R. Navarro, S. Lopez-Pedrajas, D. Luna, J.M. Marinas, F.M. Bautista, Direct hydroxylation of benzene to phenol by nitrous oxide on amorphous aluminium-iron binary phosphates, Appl. Catal. A Gen. 474 (2014) 272–279.

[28] F.M. Bautista, J.M. Campelo, A. García, D. Luna, J.M. Marinas, A.A. Romero, M.T. Siles, Vanadyl-aluminum binary phosphate: Al/V ratio influence on their structure and catalytic behavior in the 2-propanol conversion, Catal. Today. 78

(2003) 269–280.

[29] D. Lee, G. Monin, N.T. Duong, I.Z. Lopez, M. Bardet, V. Mareau, L. Gonon, G. De Paëpe, Untangling the condensation network of organosiloxanes on nanoparticles using 2D 29Si-29Si solid-state NMR enhanced by dynamic nuclear polarization, J. Am. Chem. Soc. 136 (2014) 13781–13788.

[30] F. Wijzen, B. Koch, J. Rocha, A. Esculcas, M. Liégeois-Duyckaerts, A. Rulmont, Texture and structure of amorphous co-precipitated silica-aluminum phosphate catalyst supports, J. Catal. 177 (1998) 96–104.

[31] A. Styskalik, D. Skoda, Z. Moravec, J.G. Abbott, C.E. Barnes, J. Pinkas, Synthesis of homogeneous silicophosphate xerogels by non-hydrolytic condensation reactions, Microporous Mesoporous Mater. 197 (2014) 204–212.

[32] A. Styskalik, D. Skoda, C.E. Barnes, J. Pinkas, The power of non-hydrolytic sol-gel chemistry: A review, Catalysts. 7 (2017) 168-209.

[33] W. Shen, X. Li, Y. Wei, P. Tian, F. Deng, X. Han, X. Bao, A study of the acidity of SAPO-34 by solid-state NMR spectroscopy, Microporous Mesoporous Mater. 158 (2012) 19–25.

[34] F. Blanco-Bonilla, S. Lopez-Pedrajas, D. Luna, J.M. Marinas, F.M. Bautista, Vanadium oxides supported on amorphous aluminum phosphate: Structural and chemical characterization and catalytic performance in the 2-propanol reaction, J. Mol. Catal. A Chem. 416 (2016) 105–116.

[35] S. Xu, N.R. Jaegers, W. Hu, J.H. Kwak, X. Bao, J. Sun, Y. Wang, J.Z. Hu, High-Field One-Dimensional and Two-Dimensional 27Al Magic-Angle Spinning Nuclear Magnetic Resonance Study of θ-, δ-, and γ-Al2O3Dominated Aluminum Oxides: Toward Understanding the Al Sites in γ-Al2O3, ACS Omega. 6 (2021) 4090–4099.

[36] L.A. O'Dell, S.L.P. Savin, A. V. Chadwick, M.E. Smith, A 27Al MAS NMR study of a sol-gel produced alumina: Identification of the NMR parameters of the θ-Al2O3 transition alumina phase, Solid State Nucl. Magn. Reson. 31 (2007) 169–173.

[37] F.M. Bautista, J.M. Campelo, A. Garcia, D. Luna, J.M. Marinas, A.A. Romero, A1PO4-Al2O3 catalysts with low alumina content. III. Surface basicity of

catalysts obtained in aqueous ammonia, Catal. Letters. 19 (1993) 137–142.

[38] R. Roldán, M. Sánchez-Sánchez, G. Sankar, F.J. Romero-Salguero, C. Jiménez-Sanchidrián, Influence of pH and Si content on Si incorporation in SAPO-5 and their catalytic activity for isomerisation of n-heptane over Pt loaded catalysts, Microporous Mesoporous Mater. 99 (2007) 288–298.

[39] L. Schreyeck, J. Stumbe, P. Caullet, J.C. Mougenel, B. Marler, The diaza-polyoxa-macrocycle "Kryptofix222" as a new template for the synthesis of LTA-type AlPO4: Co-templating role of F- and/or (CH3)4N+ ions, Microporous Mesoporous Mater. 22 (1998) 87–106.

[40] M.D. González, P. Salagre, E. Taboada, J. Llorca, E. Molins, Y. Cesteros, Sulfonic acid-functionalized aerogels as high resistant to deactivation catalysts for the etherification of glycerol with isobutene, Appl. Catal. B Environ. 136–137 (2013) 287–293.

[41] J. Cihlář, Hydrolysis and polycondensation of ethyl silicates. 1. Effect of pH and catalyst on the hydrolysis and polycondensation of tetraethoxysilane (TEOS), Colloids Surfaces A Physicochem. Eng. Asp. 70 (1993) 239–251.

[42] X. Li, Y. Jiang, R. Zhou, Z. Hou, Acetalization of glycerol with acetone over appropriately-hydrophobic zirconium organophosphonates, Appl. Clay Sci. 189 (2020) 105555.

a)

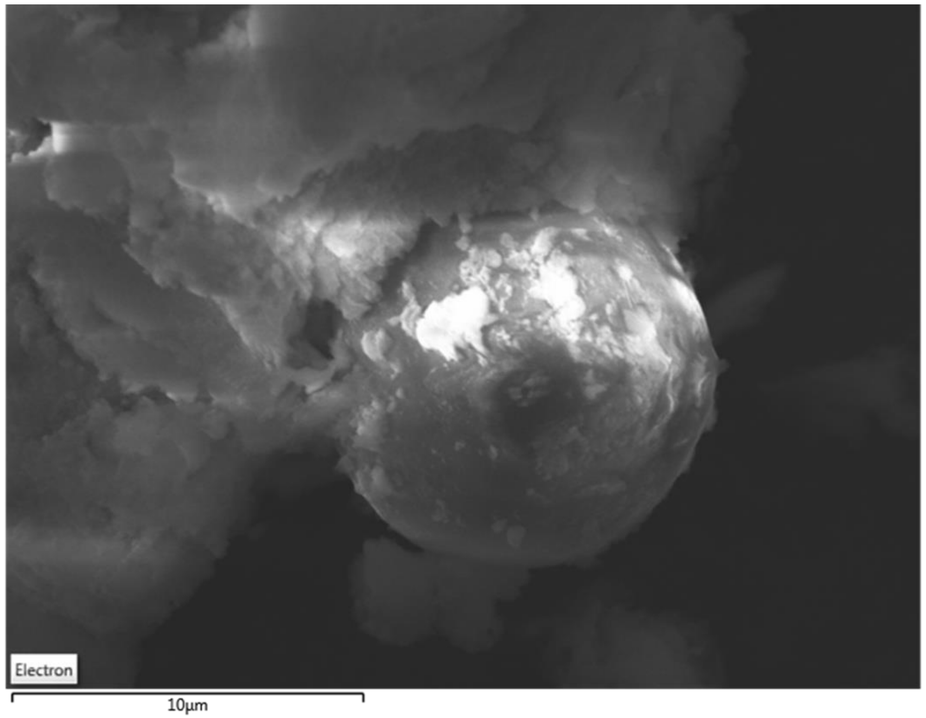


b)

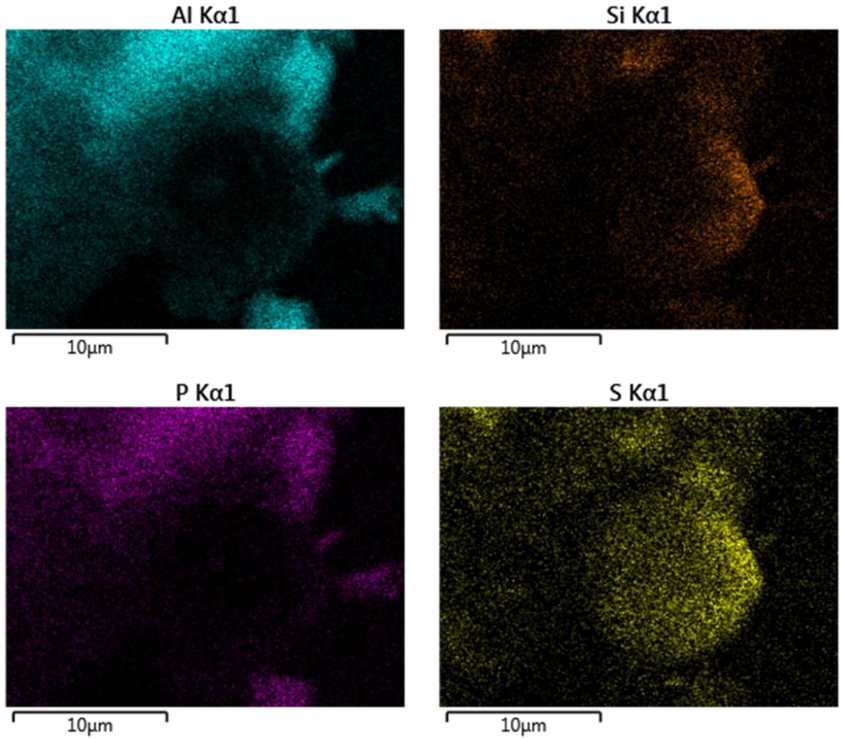


**Figure 1**

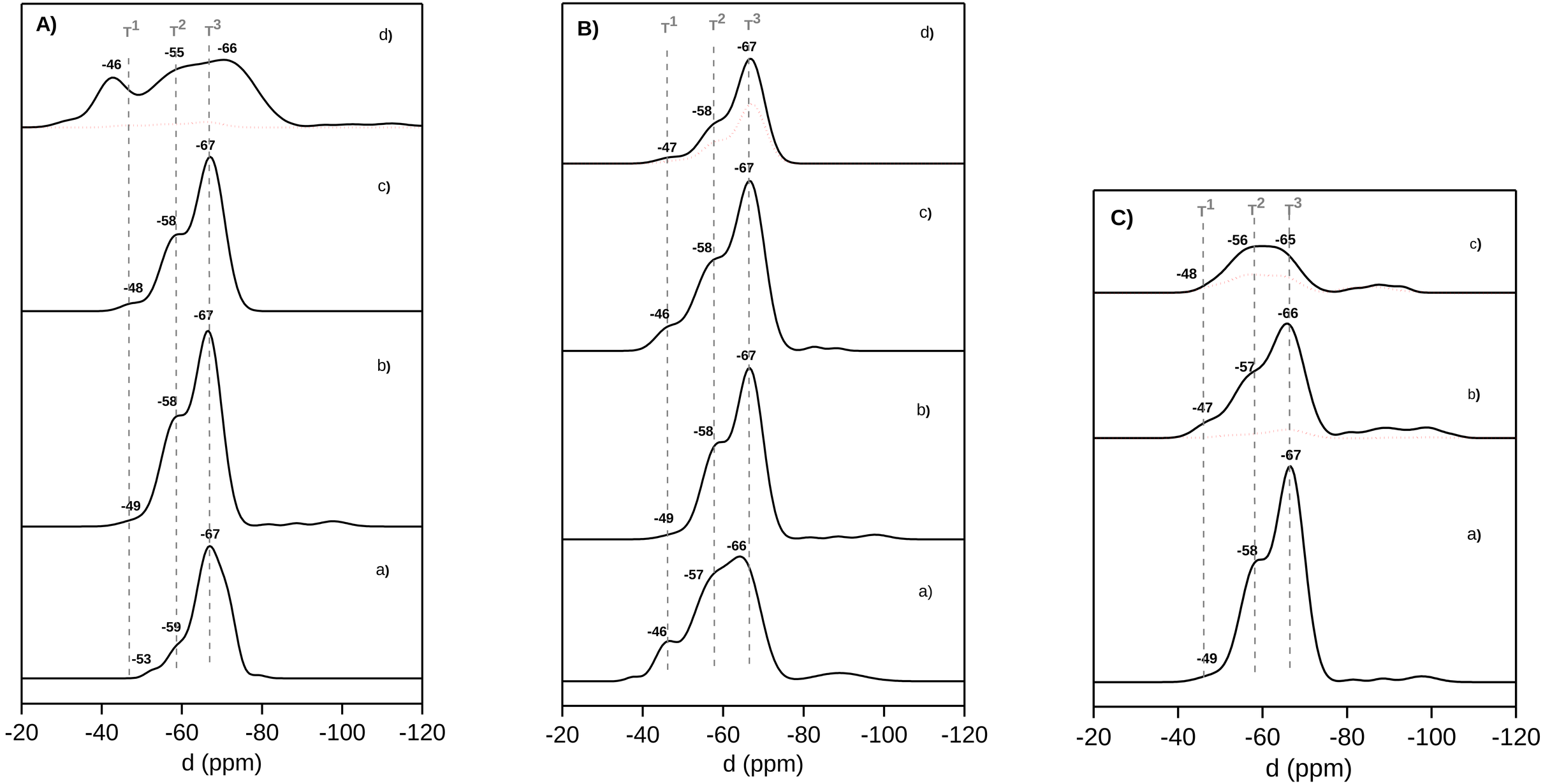
A)
T1
T2
T3
d)
-46
-55
-66
c)
-67
-58
-48
b)
-67
-58
-49
a)
-67
-59
-53
-20
-40
-60
-80
-100
-120
d (ppm)
B)
T1
T2
T3
d)
-67
-58
-47
c)
-67
-58
-46
b)
-67
-58
-49
a)
-66
-57
-46
-20
-40
-60
-80
-100
-120
d (ppm)
C)
T1
T2
T3
c)
-56
-65
-48
b)
-66
-57
-47
a)
-67
-58
-49
-20
-40
-60
-80
-100
-120
d (ppm)

**Figure 2**

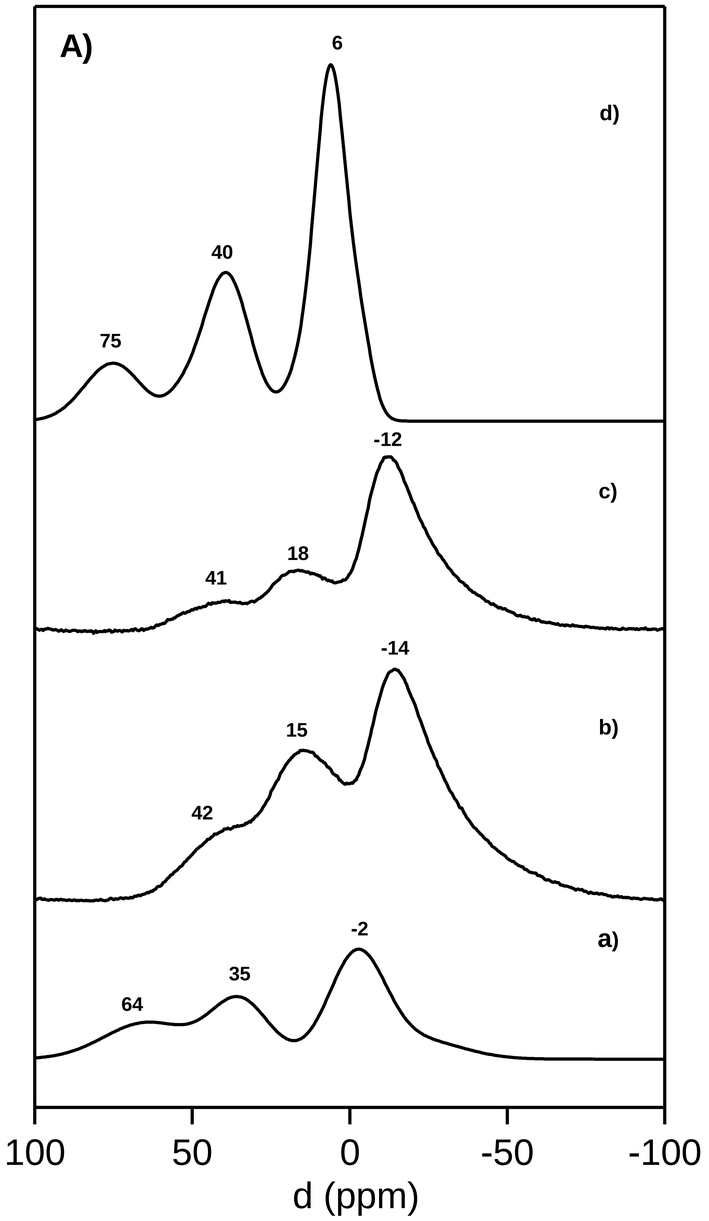
A)
d)
6
40
75
c)
-12
41
18
b)
-14
15
42
a)
-2
35
64
100
50
0
-50
-100
d (ppm)

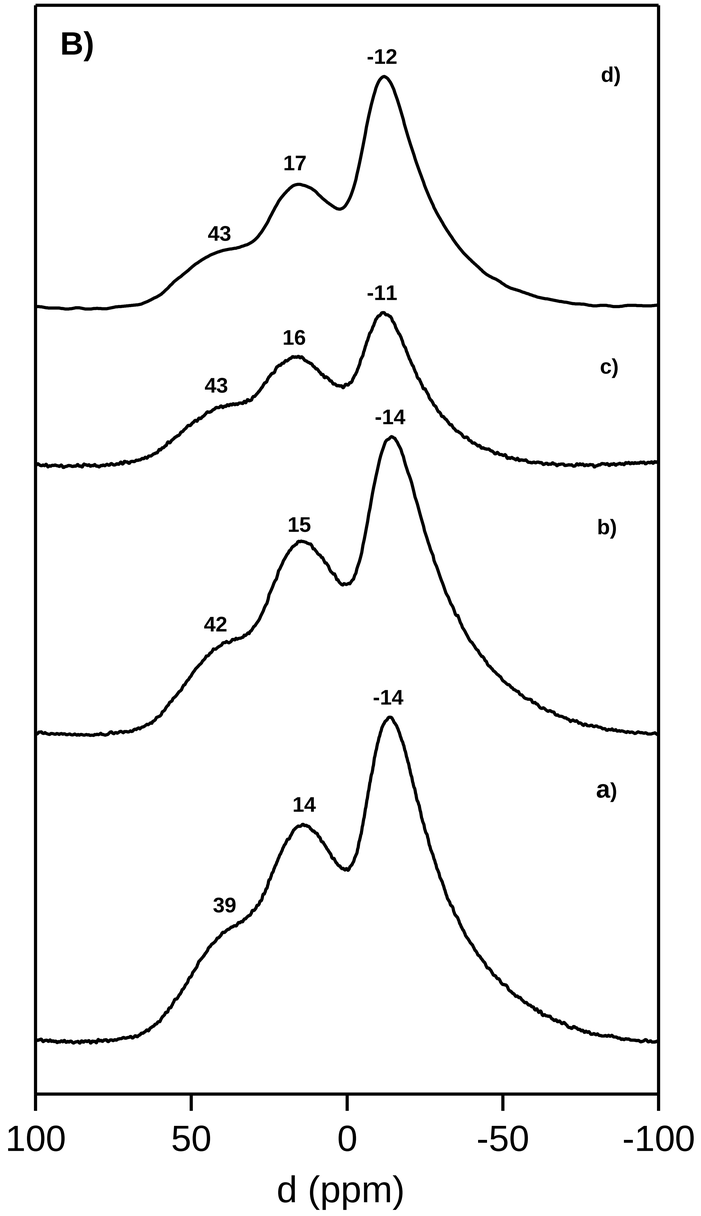
B)
d)
-12
17
43
c)
-11
16
43
b)
-14
15
42
a)
-14
14
39
100
50
0
-50
-100
d (ppm)

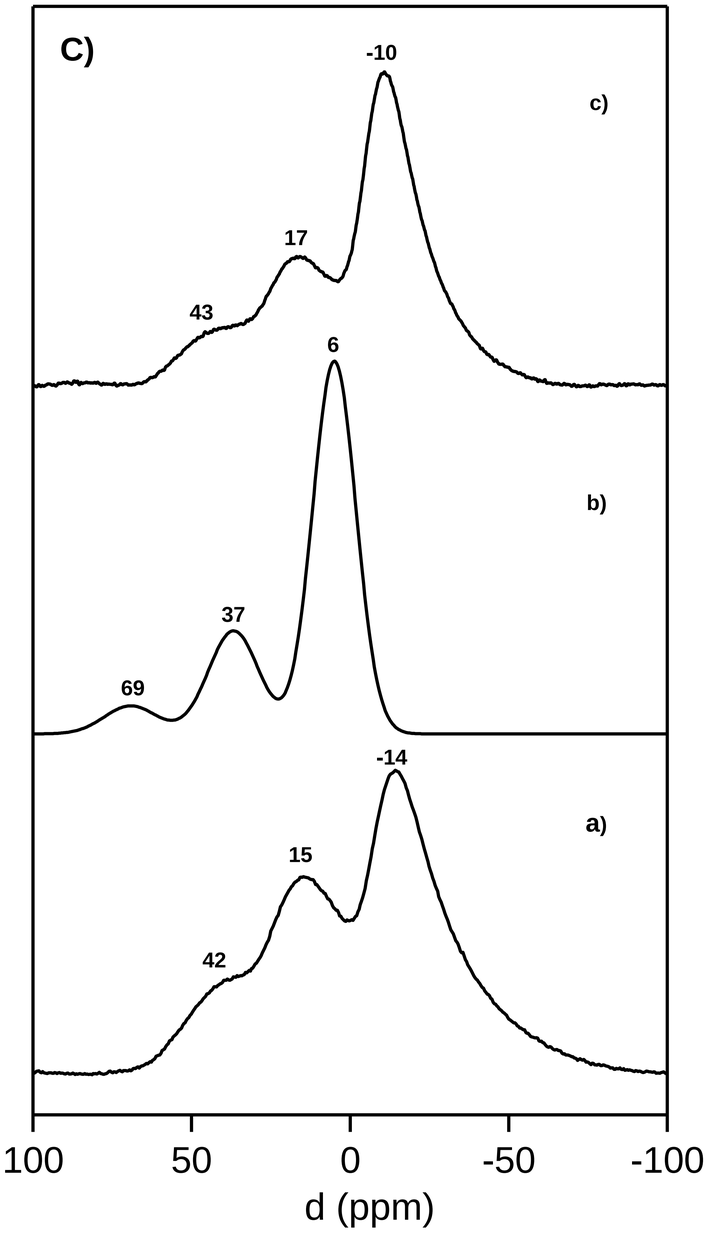
C)
c)
-10
17
43
b)
6
37
69
a)
-14
15
42
100
50
0
-50
-100
d (ppm)

**Figure 3**

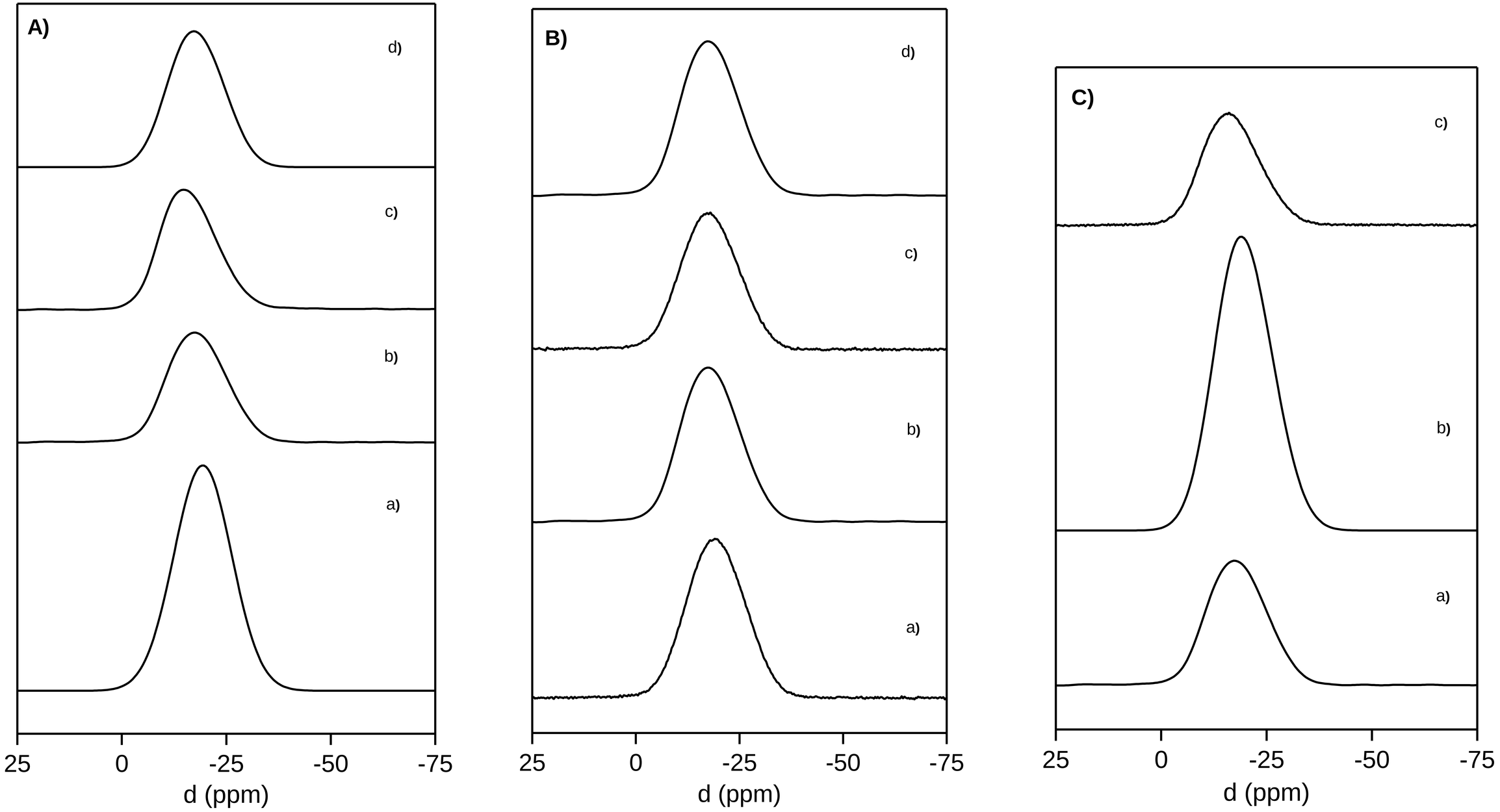
A)
d)
c)
b)
a)
25
0
-25
-50
-75
d (ppm)
B)
d)
c)
b)
a)
25
0
-25
-50
-75
d (ppm)
C)
c)
b)
a)
25
0
-25
-50
-75
d (ppm)

**Figure 4**

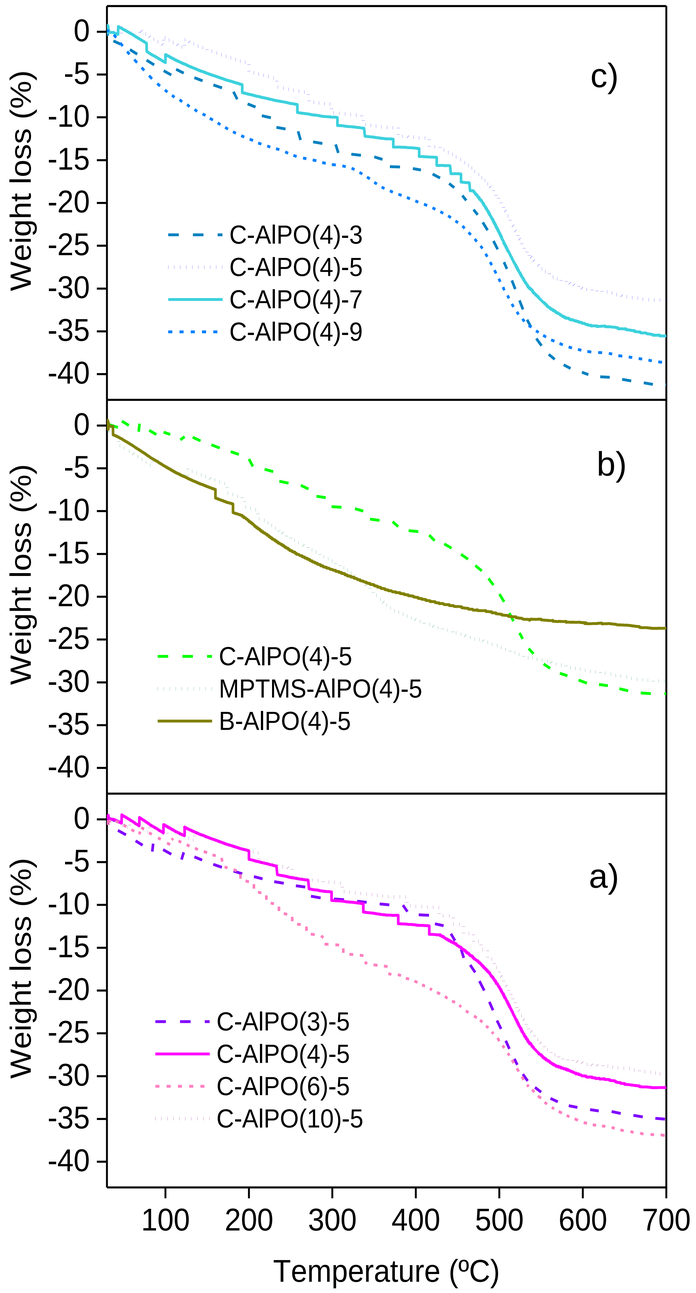
c)
C-AlPO(4)-3
C-AlPO(4)-5
C-AlPO(4)-7
C-AlPO(4)-9
b)
C-AlPO(4)-5
MPTMS-AlPO(4)-5
B-AlPO(4)-5
a)
C-AlPO(3)-5
C-AlPO(4)-5
C-AlPO(6)-5
C-AlPO(10)-5
Weight loss (%)
0
-5
-10
-15
-20
-25
-30
-35
-40
100
200
300
400
500
600
700
Temperature (ºC)

**Figure 5**

- **Figure 1.** SEM picture (a) and SEM-EDX analysis (b) of C-AlPO(4)-9. The bar indicates 10 µm.
- **Figure 2.** $^{1}H$–$^{29}Si$ CP MAS NMR spectra for the organosilica-aluminum phosphates based on the Al/P molar ratio (A): a) C-AlPO(3)-5, b) C-AlPO(4)-5, c) C-AlPO(6)-5 and d) C-AlPO(10)-5; the final pH (B): a) C-AlPO(4)-3, b) C-AlPO(4)-5, c) C-AlPO(4)-7 and d) C-AlPO(4)-9; and the organosilicon precursor (C): a) C-AlPO(4)-5, b) MPTMS-AlPO(4)-5 and c) B-AlPO(4)-5. Dotted red lines are related to $^{29}Si$ MAS NMR.
- **Figure 3.** $^{27}Al$ NMR spectra for the organosilica-aluminum phosphates based on the Al/P molar ratio (A): a) C-AlPO(3)-5, b) C-AlPO(4)-5, c) C-AlPO(6)-5 and d) C-AlPO(10)-5; the final pH (B): a) C-AlPO(4)-3, b) C-AlPO(4)-5, c) C-AlPO(4)-7 and d) C-AlPO(4)-9; and the organosilicon precursor (C): a) C-AlPO(4)-5, b) MPTMS-AlPO(4)-5 and c) B-AlPO(4)-5.
- **Figure 4.** $^{31}P$ NMR spectra for the organosilica-aluminum phosphates based on the Al/P molar ratio (A): a) C-AlPO(3)-5, b) C-AlPO(4)-5, c) C-AlPO(6)-5 and d) C-AlPO(10)-5; on the final pH (B): a) C-AlPO(4)-3, b) C-AlPO(4)-5, c) C-AlPO(4)-7 and d) C-AlPO(4)-9; and on the organosilicon precursor (C): a) C-AlPO(4)-5, b) MPTMS-AlPO(4)-5 and c) B-AlPO(4)-5.
- **Figure 5.** TG analysis for the organosilica-aluminum phosphates obtained at different synthesis conditions: Al/P molar ratio (a), type organosilica precursor (b) and final pH (c).

**Table 1.** Values of the Al/P molar ratio, silicon content (respect to the theoretical one), acidity and textural properties obtained for all the solids studied.

| Entry | Catalyst | Composition | | | Acidity | | Textural properties | | |
|---|---|---|---|---|---|---|---|---|---|
| | | Al/P molar ratio[a] | Si (%)[b] | Si (mmol/g)[a] | S (mmol S/g)[a] | Acidity (mmol $SO_3H$/g)[c] | $S_{BET}$ ($m^2$/g) | Vp ($cm^3$/g) | Mesopores (%) |
| 1 | C-AlPO(3)-5 | 3.8(4.1)[f] | 92 | 1.6 | 1.6 | 1.3 | 93 | 0.50 | 82 |
| 2 | C-AlPO(4)-5 | 4.9 | 60 | 1.4 | 1.4 | 1.0 | 82 | 0.42 | 76 |
| 3 | C-AlPO(6)-5 | 6.2(6.7) | 67 | 1.4 | 1.4 | 1.0 | 51 | 0.20 | 56 |
| 4 | C-AlPO(10)-5 | 10.5(10.6) | 49 | 1.4 | 1.4 | 1.1 | 3 | 0.14 | 1 |
| 5 | C-AlPO(4)-3 | 4.7 | 40 | 1.1 | 1.1 | 1.3 | 3 | 0.11 | 14 |
| 6 | C-AlPO(4)-7 | 4.5 | 58 | 1.4 | 1.4 | 1.2 | 170 | 0.47 | 96 |
| 7 | C-AlPO(4)-9 | 4.7(5.0) | 47 | 1.2 | 1.2 | 1.1 | 190 | 0.43 | 97 |
| 8 | MPTMS-AlPO(4)-5 | 4.1 | 60 | 1.6 | 1.4 (80%)[e] | 0.9 | 76 | 0.60 | 72 |
| 9 | B-AlPO(4)-5 | 4.3 | 11 | 0.5 | 0.4 (100%)[e] | 0.5 | 119 | 0.36 | 81 |
| 10 | C-AlPO(6)-6 | 6.6 | 77 | 1.6 | 1.6 | 1.4 | 70 | 0.38 | 90 |
| 11 | Si-Al | - | 52 | 1.5 | 1.5 | 1.3 | 25 | 0.18 | 20 |

a. Determined by X-Ray Fluorescence Spectroscopy (XRF).

b. Percentage of incorporated silicon with respect to the theoretical amount of silicon employed in the synthesis.

c. mmol of organic sulfonic group/g sample determined by Thermogravimetric Analysis (ATG).

d. Data taken from citation (Appl Catal B).

e. Percentage of oxidized sulfur (related to the total S content), determined by deconvolution of the XPS spectra.

f. Surface composition obtained from Scanning Electron Microscopy (SEM).

**Table 2**. $^{1}H–^{29}Si$ CP, $^{27}Al$, $^{31}P$ MAS NMR isotropic chemical shifts

| δ (ppm) | | | | | | | |
|---|---|---|---|---|---|---|---|
| Catalyst | $^{1}H–^{29}Si$ CP | | | $^{27}Al$ MAS | | | $^{31}P$ MAS |
| | $T^3$ | $T^2$ | $T^1$ | $Al_T$ | $Al_P$ | $Al_O$ | |
| C-AlPO(3)-5 | -67*(86)*[a] | -59*(12)* | -53*(2)* | 64*(25)* | 35*(24)* | -2*(51)* | -19*(100)* |
| C-AlPO(4)-5 | -67*(62)* | -58*(35)* | -49*(3)* | 42*(9)* | 15*(32)* | -14*(59)* | -26*(26)*; -18*(53)*; -12*(21)* |
| C-AlPO(6)-5 | -67*(66)* | -58*(31)* | -48*(3)* | 41*(8)* | 18*(23)* | -12*(69)* | -26*(15)*; -15*(85)* |
| C-AlPO(10)-5 | -66*(43)* | -55*(38)* | -46*(19)* | 75*(17)* | 40*(27)* | 6*(56)* | -23*(32)*; -15*(68)* |
| C-AlPO(4)-3 | -66*(46)* | -57*(45)* | -46*(9)* | 39*(17)* | 14*(31)* | -14*(52)* | -26*(24)*; -19*(51)*; -12*(25)* |
| C-AlPO(4)-7 | -67*(54)* | -58*(40)* | -46*(6)* | 43*(18)* | 16*(35)* | -11*(47)* | -27*(14)*; -19*(52)*; -13*(34)* |
| C-AlPO(4)-9 | -67*(67)* | -58*(29)* | -47*(4)* | 43*(11)* | 17*(31)* | -12*(58)* | -28*(7)*; -16*(93)* |
| M-AlPO(4)-5 | -66*(60)* | -57*(34)* | -47*(6)* | 69*(6)* | 37*(23)* | 6*(71)* | -21*(80)*; -15*(20)* |
| B-AlPO(4)-5 | -65*(42)* | -56*(56)* | -48*(2)* | 43*(10)* | 17*(26)* | -10*(64)* | -25*(23)*; -17*(54)*; -10*(23)* |
| C-AlPO(6)-6 | -67*(68)* | -58*(32)* | - | 77*(6)* | 40*(24)* | *5(70)* | -25(14); -16(86) |
| Si-Al | -68*(72)* | -59*(26)* | -56*(2)* | 75*(16)* | 40(24) | 7*(60)* | - |

**Table 3.** Catalytic behavior of the different catalysts after 15 min. Reaction conditions: 5.0 wt.% of catalyst referred to initial glycerol, TBA/G ratio = 4, reaction temperature 85 °C under microwave irradiation.

| Catalyst | $X_G$ (% mol) | $S_{MTBGs}$ (% mol) | $S_{h\text{-}GTBE}$ (%mol) | $Y_{h\text{-}GTBE}$ (% mol) | $Y_{h\text{-}GTBE}$/mmol $SO_3H \cdot g$[a] |
|---|---|---|---|---|---|
| C-AlPO(3)-5 | 77 | 81 | 19 | 14 | 11 |
| C-AlPO(4)-5 | 55 | 79 | 21 | 12 | 12 |
| C-AlPO(6)-5 | 59 | 81 | 19 | 11 | 11 |
| C-AlPO(10)-5 | 19 | 91 | 9 | 2 | 2 |
| C-AlPO(4)-3 | 14 | 91 | 9 | 1 | 1 |
| C-AlPO(4)-7 | 58 | 82 | 18 | 11 | 9 |
| C-AlPO(4)-9 | 69 | 82 | 18 | 13 | 12 |
| MPTMS-AlPO(4)-5 | 28 | 85 | 15 | 4 | 4 |
| BTEPTS-AlPO(4)-5 | 18 | 92 | 8 | 1 | 2 |
| C-AlPO(6)-6 | 97 | 82 | 18 | 17 | 12 |
| Si-Al | 35 | 85 | 15 | 5 | 4 |

a) mmol $SO_3H$/g has been calculated from TGA

**Table 4.** Yields to h-GTBE obtained over several solids before and after 15 min of reaction, under MW irradiation.

| Catalyst | $Y_{h\text{-}GTBE}$ (% mol) | | | | |
|---|---|---|---|---|---|
| | **Fresh** | **1st Use** | **2nd Use** | **3rd Use** | **4th Use** |
| C-AlPO(4)-5 | 12 | 11 | 8 | 5 | 8 |
| C-AlPO(6)-5 | 11 | 13 | - | - | - |
| C-AlPO(4)-7 | 11 | 11 | - | - | - |
| MPTMS-AlPO(4)-5 | 4 | 3 | - | - | - |
| C-AlPO(6)-6 | 17 | 16 | 10 | 10 | 4 (11)* |

* Yield obtained after the extraction of remained glycerol and products of the reaction.